Aalto University

OPEN ACCESS

This is an electronic reprint of the original article.
This reprint may differ from the original in pagination and typographic detail.

Ferreira, Daniela C.; Oliveira, Mayara L.; Bioni, Thais A.; Nawaz, Haq; King, Alistair W.T.; Kilpeläinen, Ilkka; Hummel, Michael; Sixta, Herbert; El Seoud, Omar A.

Binary mixtures of ionic liquids-DMSO as solvents for the dissolution and derivatization of cellulose

Published in:
Carbohydrate Polymers

DOI:
10.1016/j.carbpol.2019.02.024

Published: 15/05/2019

Document Version
Peer-reviewed accepted author manuscript, also known as Final accepted manuscript or Post-print

Published under the following license:
Unspecified

Please cite the original version:
Ferreira, D. C., Oliveira, M. L., Bioni, T. A., Nawaz, H., King, A. W. T., Kilpeläinen, I., Hummel, M., Sixta, H., & El Seoud, O. A. (2019). Binary mixtures of ionic liquids-DMSO as solvents for the dissolution and derivatization of cellulose: Effects of alkyl and alkoxy side chains. *Carbohydrate Polymers*, *212*, 206-214. https://doi.org/10.1016/j.carbpol.2019.02.024

This material is protected by copyright and other intellectual property rights, and duplication or sale of all or part of any of the repository collections is not permitted, except that material may be duplicated by you for your research use or educational purposes in electronic or print form. You must obtain permission for any other use. Electronic or print copies may not be offered, whether for sale or otherwise to anyone who is not an authorised user.

CARBPOL-D-18-04614- revised text

Binary mixtures of ionic liquids-DMSO as solvents for the dissolution and derivatization of cellulose: Effects of alkyl and alkoxy side chains

Daniela C. Ferreira[a,b], Mayara L. Oliveira[a], Thais A. Bioni[a], Haq Nawaz[a], Alistair W. T. King[c], Ilkka Kilpeläinen[c], Michael Hummel[d], Herbert Sixta[d*], Omar A. El Seoud[a*]

[a] *Institute of Chemistry, the University of São Paulo, Prof. Lineu Prestes Av., 748, 05508-000, São Paulo, SP; Brazil*

[b] *Institute for Technological Research from State of São Paulo, Prof. Almeida Prado Av., 532, 05508-901, São Paulo, SP, Brazil*

[c] *Department of Chemistry, University of Helsinki A.I. Virtasen Aukio 1, 00014, P.O. Box 55, Helsinki, Finland*

[d] *Department of Bioproducts and Biosystems, School of Chemical Engineering, Aalto University, P.O. Box 16300, FI-00076 Aalto, Finland*

*herbert.sixta@aalto.fi, +358 50 3841 764

*elseoud.usp@gmail.com, +55 11 3091 3874

Abstract

The efficiency of mixtures of ionic liquids (ILs) and molecular solvents in cellulose dissolution and derivatization depends on the structures of both components. We investigated the ILs 1-(1-butyl)-3-methylimidazolium acetate (C_4MeImAc) and 1-(2-methoxyethyl)-3-methylimidazolium acetate (C_3OMeImAc) and their solutions in dimethyl sulfoxide, DMSO, to assess the effect of presence of an ether linkage in the IL side-chain. Surprisingly, C_4MeImAc-DMSO was more efficient than C_3OMeImAc-DMSO for the dissolution and acylation of cellulose. We investigated both solvents using rheology, NMR spectroscopy, and solvatochromism. Mixtures of C_3OMeImAc-DMSO are more viscous, less basic, and form weaker hydrogen bonds with cellobiose than C_4MeImAc-DMSO. We attribute the lower efficiency of C_3OMeImAc to "deactivation" of the ether oxygen and C2-***H*** of the imidazolium ring due to intramolecular hydrogen bonding. Using the corresponding ILs with C2-***CH_3*** instead of C2-***H***, namely, 1-butyl-2,3-dimethylimidazolium acetate (C_4Me_2ImAc) and 1-(2-methoxyethyl)-2,3-dimethylimidazolium acetate (C_3OMe_2ImAc) increased the concentration of dissolved cellulose; without noticeable effect on biopolymer reactivity.

Keywords: *ionic liquid-DMSO; cellulose dissolution; solvatochromism; biopolymer derivatization; cellulose esters.*

1. Introduction

There is sustained interest in investigating solvents for the physical dissolution of cellulose, i.e., without formation of covalent bonds. The reason is that the resulting solutions are used for cellulose regeneration in different forms, including fibers (Jedvert & Heinze, 2017) and nanospheres (Gericke, Trygg, & Fardim, 2013), and for synthesizing cellulose derivatives - in particular esters - with controlled properties (El Seoud, Nawaz, & Arêas, 2013; Gericke, Liebert, El Seoud, & Heinze, 2011). Cellulose fiber regeneration from its solutions is commercially important because cotton production is not expected to meet world population demand for cellulosic fibers by 2030 (Hämmerle, 2011). The viable solution to close this so-called "cellulosic fiber gap" is to increase cellulose use from sources other than cotton (e.g., wood and agricultural residues) and enhance the efficiency of recycling, e.g., of cellulose-containing fabrics (Eichinger, 2012).

The solvent employed should disrupt the intramolecular hydrogen bonds within the anhydrous glucose unit (AGU), the intermolecular hydrogen bonds between the biopolymer chains, and the van der Waals interactions present because cellulose is amphiphilic and has a relatively hydrophobic inner surface (Lindman et al., 2017; Medronho, Romano, Miguel, Stigsson, & Lindman, 2012). Consequently, efficient cellulose solvents are strongly dipolar or ionic, employed pure or as solutions in molecular solvents (MSs), usually dipolar aprotic ones. Examples are LiCl/*N,N*-dimethylacetamide, DMAc (El Seoud et al., 2013), *N*-methyl morpholine-*N*-oxide hydrate (Rosenau, Hofinger, Potthast, & Kosma, 2003); ionic liquids, ILs, based on heterocyclic rings, in particular imidazole (Gericke, Fardim, & Heinze, 2012; Laus et al., 2005) and quaternary ammonium electrolytes (QAE)/MSs (Casarano, Nawaz, Possidonio, Da Silva, & El Seoud, 2011; Heinze et al., 2000; Kostag, Jedvert, Achtel, Heinze, & El Seoud, 2018).

Figure 1 shows a schematic representation of the mechanism of cellulose dissolution in QAE/MS where, for simplicity, the steps are depicted as occurring in sequence; this need not be the case. Part (a) of Figure 1 shows the cellulose chains immersed in the MS (blue background) before the introduction of the QAE; in (b) the anion interacts with the hydroxyl groups of the AGU. The chains are separated by electrostatic repulsion because they acquire a negative charge.

As shown in part (c), the solvated polymer chains are further separated, i.e., the biopolymer-QAE complex dissolves in the MS because of "condensation" of the (voluminous) cation around the biopolymer-anion complex (Östlund, Lundberg, Nordstierna, Holmberg, & Nydén, 2009; Papanyan, Roth, Wittler, Reimann, & Ludwig, 2013; Wei, Meng, Cui, Jiang, & Zhou, 2017).

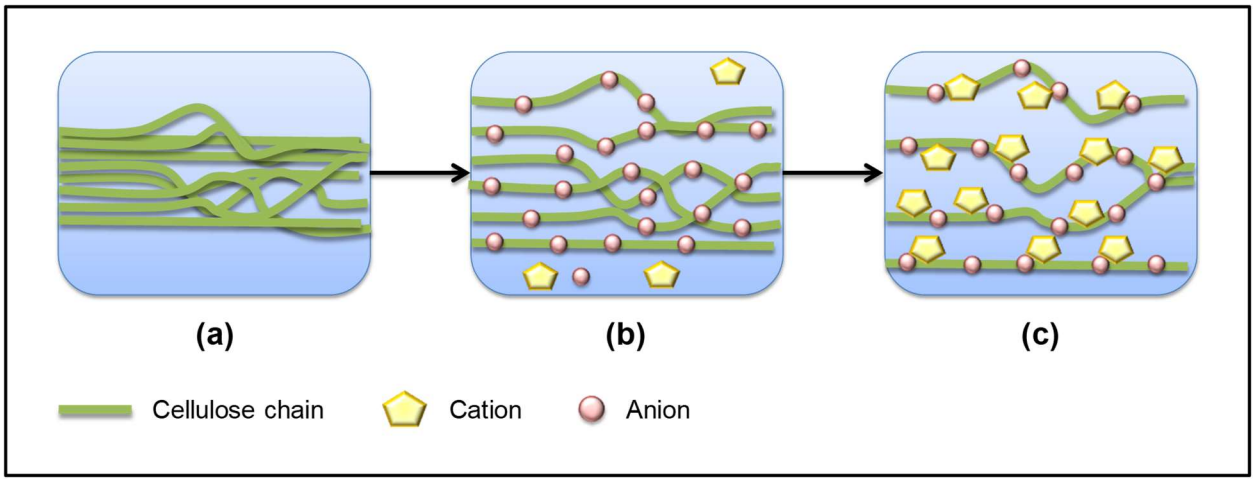

Figure 1. Schematic representation of cellulose dissolution in quaternary ammonium electrolytes/molecular solvent mixture: (a) cellulose (green lines) is added to the MS (blue background); (b) the anions (pinkish spheres) interact with the hydroxyl groups of cellulose (polar domains) which separate the cellulose chains because they acquire a negative charge; in (c) the cations (yellow pentagrams) join the anions and separate entirely the cellulose chains leading to its dissolution.

Therefore, cellulose dissolution is a function of the charge density (or hardness) of the ions and their volumes, both determine anion-cation, ion-cellulose and, where applicable, ion-MS interactions. In the present study, we used solutions in DMSO of the ILs shown in Figure 2 for the dissolution and acylation of microcrystalline cellulose, MCC. The IL anion was acetate and the corresponding cations differ in the presence of an ether oxygen in the side chain, and of hydrogen or methyl group in position 2 of the imidazolium ring.

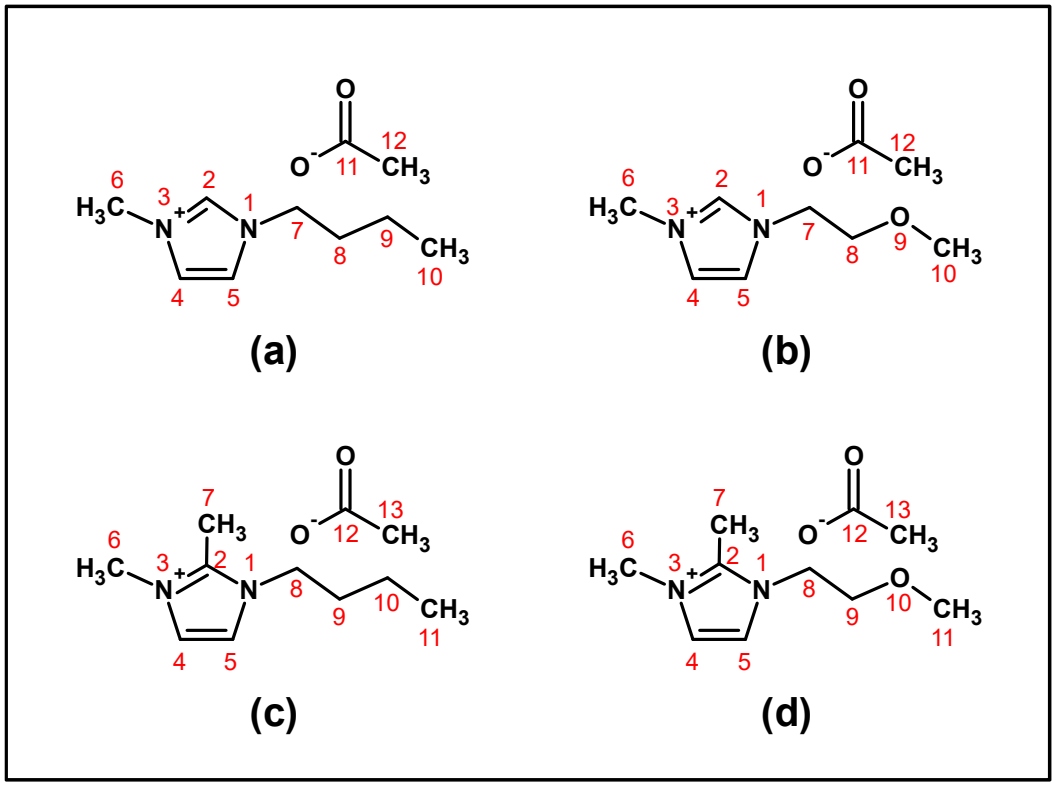

Figure 2. Molecular structures of the studied ionic liquids: (a) 1-(1-butyl)-3-methylimidazolium acetate (C_4MeImAc); (b) 1-(2-methoxyethyl)-3-methylimidazolium acetate (C_3OMeImAc); (c) 1-(1-butyl)-2,3-dimethylimidazolium acetate (C_4Me_2ImAc); and (d) 1-(2-methoxyethyl)-2,3-dimethylimidazolium acetate (C_3OMe_2ImAc). The atoms are numbered in red.

The presence of an ether oxygen resulted in more viscous IL and IL- DMSO mixtures; lower effective basicity, and lower degree of substitution, *DS* of the synthesized acetate and benzoate esters. We attribute these results to "deactivation" of the ether group and the C2-***H*** of the imidazolium ring due to intramolecular hydrogen bonding. "Blocking" of the C2 position of the heterocyclic ring increased cellulose dissolution in the IL-DMSO mixtures but reflected little on cellulose reactivity.

2. Experimental Section

2.1. Chemicals

The chemicals were purchased from Sigma-Aldrich or Merck and were purified as recommended elsewhere (Armarego & Chai, 2009). Microcrystalline cellulose (MCC), Avicel PH 101 (viscosity-based degree of polymerization $\overline{DP}_V$ = 175) was from Sigma-Aldrich and kraft dissolving eucalyptus pulp ($\overline{DP}_V$ = 497) was from Bahia Specialty, Salvador. The solvatochromic probes employed (Figure 3) were previously synthesized as reported elsewhere (Catalán et al., 1996; Catalan, Mena, Meutermans, & Elguero, 1992).

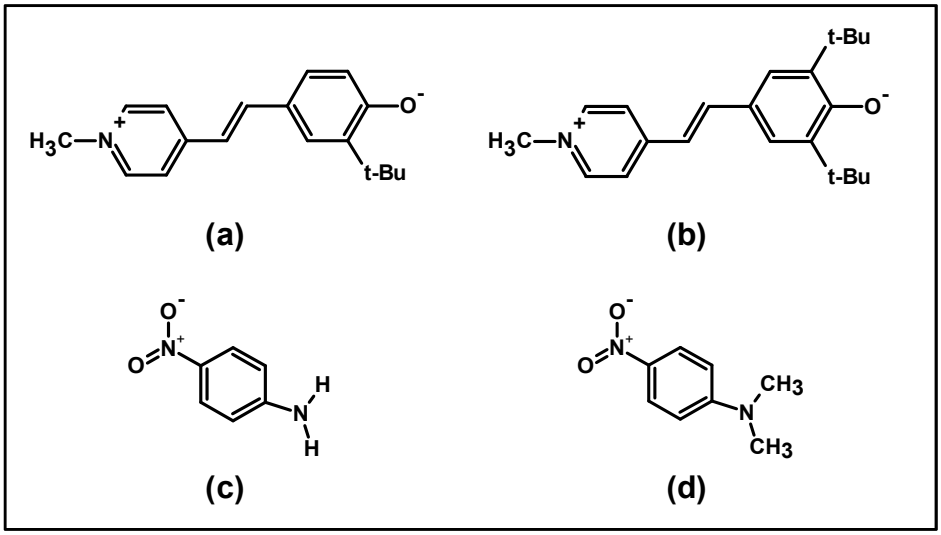

Figure 3. Molecular structure of the solvatochromic probes employed. (a) *o*-tert-butylstilbazolium betaine (TBSB); (b) *o,o´*-di-tert-butylstilbazolium betaine (DTBSB); (c) 4-nitroaniline (NA); (d) *N,N*-dimethyl-4-nitroaniline (DMNA).

2.2. Equipment

NMR spectroscopic data were obtained with Varian, Inova 300 (300 MHz for ^{1}H), or Bruker DRX 500 (500 MHz for ^{1}H) spectrometers. The UV-VIS spectra of the solvatochromic probes were recorded with Shimadzu UV-2550 spectrophotometer. The temperature inside the cuvette holder was controlled $\pm$ 0.05 ^{o}C with a digital thermometer (Yellow Springs Instruments model 4000A). The rheology data were acquired with Physica model MCR 300 rheometer (Anton Paar) with cone-plate geometry (50 cm diameter) using Peltier heating element ($\pm$ 0.1 ^{o}C) and Rheoplus software.

We dissolved MCC in the IL-DMSO by continuous magnetic stirring in a glass tube with GL 25 threaded polybutylene terephthalate (PBT) screw cap (DURAN®), provided with an inner PTFE protecting seal, and evaluated the dissolution under 12x magnifying glass provided with LED light, followed by examination under a microscope (Nikon, Eclipse 2000 microscope with cross polarization) as given elsewhere (Kostag & El Seoud, 2019). We carried out cellulose acylation as given elsewhere, (Possidonio, Fidale, & El Seoud, 2009) employing Discover model DU-8316 (CEM) microwave equipment and IKA model RW 20 mechanical stirrer with a digital tachometer.

2.3. Synthesis of C_4Me_nImAc and C_3OMe_nImAc (n = 1 or 2)

Four ionic liquids were prepared: 1-(1-butyl)-3-methylimidazolium acetate (C_4MeImAc); 1-(1-butyl)-2,3-dimethylimidazolium acetate (C_4Me_2ImAc); 1-(2-methoxyethyl)-3-methylimidazolium acetate (C_3OMeImAc); and 1-(2-methoxyethyl)-2,3-dimethylimidazolium acetate (C_3OMe_2ImAc). Figure 2 shows the molecular structures of these ILs along with the corresponding atoms numbering.

The ILs were synthesized as described elsewhere (El Seoud et al., 2011) and schematized in Figure 4. In a typical run, the appropriate volumes of the reagents (see Table 1) were charged into PTFE-coated stainless-steel reactor and heated at 110 °C for 6 h under constant stirring and pressure (N_2, 10 bar). After cooling to room temperature and removal of acetonitrile, the IL (as chloride; ($IL-Cl^-$)) was purified by vigorously stirring with cold ethyl acetate (three times, 75 mL each time); separated (lower layer) and dried at 40 °C under reduced pressure over P_4O_{10} for 72 h. The $IL-OAc^-$ was obtained by anion exchange ($IL-Cl^- \rightarrow IL-OH^-$; methanol solvent), followed by neutralization of the $IL-OH^-$ with acetic acid. The completeness of the (Cl^-/OH^-) ion-exchange was assured by testing a dilute aqueous solution of the $IL-OH^-$ with $AgNO_3/HNO_3$ solution. After neutralization, methanol was evaporated under reduced pressure and the IL was dried at 40 °C under reduced pressure over P_4O_{10} for 96 h. The final yield for each IL is shown in Table 1. The structure of the IL was confirmed by ^{1}H NMR spectroscopy (Table SM1, Table 1 of supplementary material).

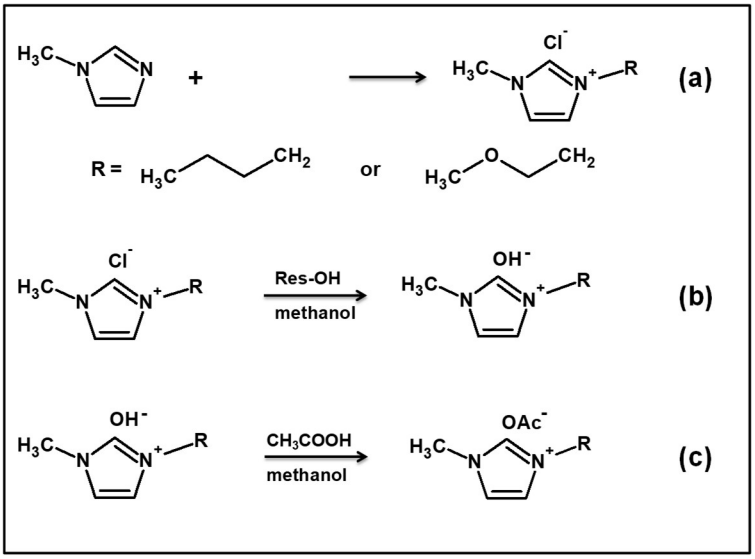

Figure 1. Synthesis of IL: (a) preparation of IL in the chloride form; (b) Cl^-/OH^- ion exchange ($IL - Cl^-$); (c) neutralization of $IL - OH^-$ with acetic acid ($IL - OAc^-$).

Table 1. Synthesis conditions and properties of the ionic liquids employed

Ionic Liquid	1-Methylimidazole		Alkyl or alkoxy chloride		CH_3CN, mL	IL yield, %[c]
	Compound[a]	g (mole)	Compound[b]	g (mole)		
C_4MeImAc	*A*	38.7 (0.50)	C	47.3 (0.45)	150	79
C_4Me_2ImAc	*B*	38.7 (0.50)	C	47.3 (0.45)	150	97
C_3OMeImAc	*A*	23.4 (0.30)	D	29.5 (0.27)	55	92
C_3OMe_2ImAc	*B*	23.4 (0.30)	D	29.5 (0.27)	55	97

[a] A = *N*-methylimidazole; B= *1,2*-dimethylimidazole;

[b] C = *1*-chlorobutane; D = *1*-chloro-*2*-methoxyethane;

[c] IL yield (%) = ($n_{alkyl\ or\ alkoxy\ chloride}/n_{IL}$) x 100, where *n* = number of mol of the indicated substance.

2.4. Cellulose dissolution

We evaluated MCC dissolution in pure RMe_nImAc (n = 1 and 2) and binary mixtures of

RMe$_n$ImAc-DMSO with DMSO at a mole fraction (χ_{DMSO}) between 0.2 and 0.9. In a typical experiment, we introduced the solvent (pure or binary mixture, *ca.* 2 g) into the above-mentioned glass vial, heated it to 60 ^oC under continuous magnetic stirring for 15 min. We added a small mass of MCC (*ca.* 5-10 mg; dried at 60 ^oC; reduced pressure; 8 h) to the heated solvent and continued the stirring for additional 15 min. We evaluated the solubility of cellulose as indicated above. If a dark image was observed in the microscope, we considered the cellulose soluble, added fresh cellulose and repeated the stirring/examination protocol. If we observed luminous spots in the image, due to (undissolved) cellulose crystals, we heated/stirred the mixture at 60 ^oC for an additional hour and assessed the solubility. We continued this protocol until cellulose did not dissolve after 75 minutes of the last biopolymer addition; we considered, arbitrarily, that this is the saturation point. We report the dissolved cellulose in wt % as shown below. We employed a similar procedure for eucalyptus pulp at a single solvent composition where the maximum solubility of MCC was observed.

$$\textit{Cellulose solubility}, \text{ wt\%} = (m_{Cellulose}/\ m_{Cellulose} + m_{Solvent}) \times 100 \quad \textbf{(1)}$$

where, $m_{Cellulose}$ is the total mass of dissolved cellulose; $m_{Solvent}$ is the initial mass of solvent.

2.5. Acylation of MCC in RMe$_n$ImAc-DMSO using *N*-acyl imidazole

Cellulose acetate (Cell-Ac) and cellulose benzoate (Cell-Bz) were synthesized as described elsewhere (Possidonio et al., 2009) using *N*-acylimidazole synthesized *in situ*. Firstly, an MCC (0.5 g MCC, 3.1 mmol) solution in RMe$_n$ImAc-DMSO (10 g of IL-DMSO, χ_{DMSO} =0.7) was prepared by heating the suspension in a MW-equipment for 10 min (30 W nominal power; 80 ^oC; mechanical stirring, 500 rpm). In another reaction flask, *N*-acyl imidazole was synthesized by reacting acetic anhydride (0.44 mL, 4.6 mmol) or benzoic anhydride (1.05 g, 4.6 mmol) and imidazole (0.66 g, 9.2 mmol) in 2 mL of DMSO by stirring at room temperature for 30 min.

The *N*-acyl imidazole suspension in DMSO was added, in one portion, to the MCC-RMe$_n$ImAc-DMSO solution and the reaction mixture (χ_{DMSO} 0.6) was heated under MW-irradiation with mechanical stirring (2 h; 60 ^oC; 15 W power; 500 rpm). The cellulose ester was

isolated by precipitation in ethanol (70 mL) and washing five times with warm ethanol (50 mL each wash, 40 °C). The degree of substitution of Cell-Ac (DS_{Ac}) and Cell-Bz (DS_{Bz}) was determined by integration of ^{1}H NMR spectra (300 MHz) obtained from cellulose ester solution in DMSO-d_6 (~ 33 mg/mL), containing 2-3 drops of trifluoroacetic acid. The calculations of *DS* are indicated in item 3 of SM; the uncertainty in *DS* was ≤ 0.05.

2.6. Viscosity measurements of ILs and ILs-DMSO

The flow curves of pure RMeImAc and binary RMeImAc-DMSO mixtures with $0.0 < \chi_{DMSO} < 1.0$, were examined at (60 $\pm$ 0.05) °C using 90 s^{-1} shear rate (cone-plate fixture, 50 cm diameter). In order to eliminate absorption of adventitious water, the plate was surrounded with home-constructed PTFE circular "trough" filled with silica gel and covered with two-part glass cover with a central hole, as shown in Figure SM2.

To calculate the energy of viscous flow, the viscosity of binary RMeImAc-DMSO mixtures, with and without dissolved MCC (1 % weight) were obtained at 40 °C, 60 °C, and 80 °C with a constant shear rate of 90 s^{-1}. The energy of viscous flow was calculated by Arrhenius-type equation, i.e., from the slope of ln(η) x 1/*T* plot. (Gericke, Schlufter, Liebert, Heinze, & Budtova, 2009).

2.7. NMR spectroscopic study of cellobiose/RMeImAc-DMSO interactions

Solutions of cellobiose (model for cellulose) in RMeImAc-DMSO-d_6 were prepared as follows: to ten small glass vials were added 200 mg of IL; 1 mL of DMSO-d_6; and increasing concentrations of cellobiose (2-25 mg). Each mixture was stirred with a magnetic bar at 40 °C for 30 min. until complete dissolution of cellobiose. The solution (0.5 mL) was transferred to NMR tube and its ^{1}H NMR and ^{13}C NMR spectra (500 MHz) were recorded at room temperature.

2.8. Spectrophotometric determination of Lewis acidity (*SA*) and Lewis basicity (*SB*) using solvatochromic dyes

We prepared binary mixtures of RMe_nImAc-DMSO (n = 1 or 2) by weight to cover a χ_{DMSO}

range of 0.2 to 0.9. We pipetted the solvatochromic probes (Figure 3) solutions in acetone (6 μg/mL) into small glass vials with a plastic cap and dried the solutions under reduced pressure over P_4O_{10}. To the glass vials containing the (solid) solvatochromic probe we added pure RMe_nImAc, pure DMSO, and binary mixtures RMe_nImAc-DMSO; and dissolved the probe at room temperature using a tube rotator (Labquake, Lab Industries; 30 min; 60 rpm). The final probe concentration was 2-5 x 10^{-4} mol/L for all probes.

UV-VIS spectra of probe solutions were recorded twice using the following parameters: scan speed of 120 nm/min; spectral resolution of 0.2 nm; 60 °C. We calculated values of λ_{max} from the first derivative curve of the absorption spectrum. The uncertainty in this determination was $\pm$ 0.5 nm. We calculated Lewis acidity (*SA*) and Lewis basicity (*SB*) from the values of λ_{max} of the intramolecular charge transition band as given in item 6 of SM.

3. RESULTS AND DISCUSSIONS

3.1. Effects of the IL side-chain structure on cellulose dissolution: C_4MeImAc versus C_3OMeImAc

We show in Figure 5a the wt% dissolved MCC at 60 °C in the pure ILs and their binary mixtures with DMSO; $\boldsymbol{\chi_{DMSO}}$ = 0.2 – 0.9 (pure DMSO causes only cellulose swelling); we comment on Figure 5b later. The maximum dissolution in both RMeImAc (R = 1-butyl or 2-methoxyethyl) occurs at the same $\boldsymbol{\chi_{DMSO}}$ = 0.6. At this molar fraction, the wt% dissolved MCC was 13 and 16 for C_3OMeImAc-DMSO and C_4MeImAc-DMSO, respectively. At $\boldsymbol{\chi_{DMSO}}$ = 0.6, the eucalyptus pulp solubility was 4.5 wt% and 6.0 wt%, for C_3OMeImAc-DMSO and C_4MeImAc-DMSO, respectively.

Therefore: (i) IL-DMSO mixtures dissolve more MCC than eucalyptus pulp; and (ii) under the same conditions, the IL with an alkyl side-chain (C_4MeImAc) dissolves more cellulose than the one with alkoxy side-chain (C_3OMeImAc). That is, we did not observe the expected beneficial effect on cellulose dissolution from the presence of ether oxygen in the side-chain of C_3OMeImAc.

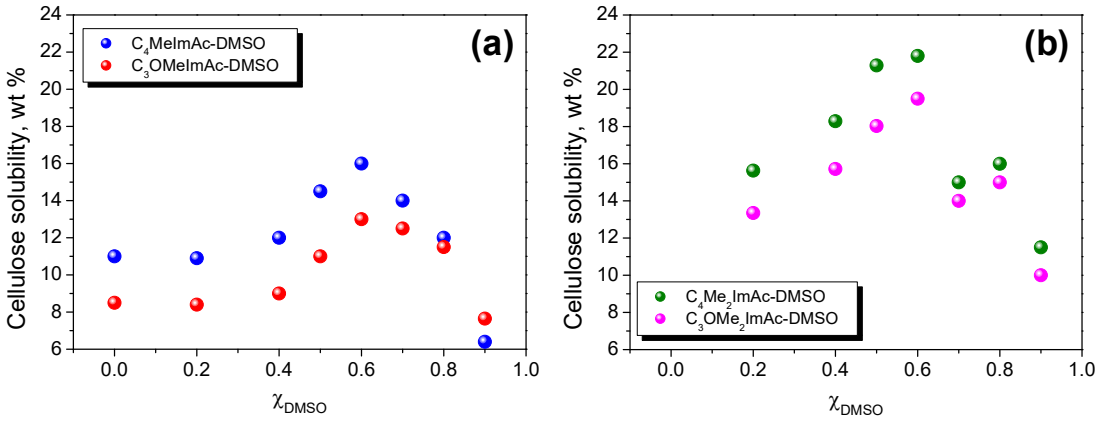

Figure 5. Dissolution curve of MCC in binary mixtures of IL-DMSO in a different molar fraction of DMSO (χ_{DMSO}) determined at 60 °C. IL = RMe$_n$ImAc, R = 1-butyl or 2-methoxyethyl, n = 1 (a) or 2 (b).

3.2. Effects of the IL side-chain structure on cellulose acylation: C$_4$MeImAc-DMSO versus C$_3$OMeImAc-DMSO

Acylation of MCC by *N*-acyl imidazole (acyl = acetyl, benzoyl) was carried in a binary mixture of RMeImAc-DMSO (χ_{DMSO} 0.6), the solvent composition of maximum solubility of MCC. We used *N*-acyl imidazoles, generated in situ by the reaction:

Acid anhydride + 2 imidazole $\rightarrow$ *N*-acyl imidazole + imidazolium carboxylate **(2)**

We used *N*-acylimidazoles rather than the parent acid anhydrides because of the side reaction between the latter and DMSO (Albright & Goldman, 1965, 1967; Marx & Tidwell, 1984; Omura & Swern, 1978). As we showed earlier, the formation of *N*-acyl imidazole is quantitative; the formed imidazolium salt has no effect on the rate of acylation, *i.e.,* it does not act as an acid/base catalyst (Nawaz, Pires, & El Seoud, 2013; Pires et al., 2015). In the acylation experiments, we were interested in assessing cellulose reactivity at its maximum dissolution because of the demonstrated cellulose aggregation in solutions of LiCl/*N,N*-dimethylacetamide and ILs (Ciacco, Morgado, Frollini, Possidonio, & El Seoud, 2010; Kuzmina, Sashina, Troshenkowa, & Wawro, 2010).

In the first four entries of Table 2 we list the values of *DS* of cellulose esters prepared in pure C_4MeImAc-DMSO and C_3OMeImAc-DMSO; we will address entries 5 and 6 later. In entries 1 to 4, values of DS_{Ac} are higher than DS_{Bz}. These results agree with previous data on MCC acylation with carboxylic acid anhydrides and *N*-acylimidazoles in tetra(*n*-butyl)ammonium fluoride hydrate/DMSO (Nagel & Heinze, 2012). Likewise, the values of DS_{Ac} and DS_{Bz} of cellulose esters prepared in C_4MeImAc-DMSO are higher than those obtained in C_3OMeImAc-DMSO. That is, the dependence of cellulose reactivity on the molecular structure of the IL (as indicated by *DS*) is parallel to its dissolution in the same media.

Table 2. Degree of substitution of cellulose esters prepared in RMe_nImAc-DMSO (χ_{DMSO} 0.6; n = 1 or 2)[a,b]

Entry	IL-MS	Acylating agent	Esters obtained	DS_{Ac}	DS_{Bz}
Ionic Liquids based on 1-methylimidazole					
1	C_4MeImAc-DMSO	*N*-acetyl imidazole	Acetate	1.64	-
2	C_3OMeImAc-DMSO	*N*-acetyl imidazole	Acetate	0.81	-
3	C_4MeImAc-DMSO	*N*-benzoylimidazole	Acetate + benzoate	0.46	1.02
4	C_3OMeImAc-DMSO	*N*-benzoylimidazole	Acetate + Benzoate	0.63	0.41
Ionic Liquids based on 1,2-dimethylimidazole					
5	C_4Me_2ImAc-DMSO	*N*-acetylimidazole	Acetate	1.10	-
6	C_3Ome_2ImAc-DMSO	*N*-acetylimidazole	Acetate	1.00	-

[a] Microwave-assisted acylation employing 15 W, 60 °C and 2 h of reaction;

[b] Molar ratio of MCC: *N*-acylimidazole = 1.0 : 1.5.

The ^{1}H NMR spectra of the obtained cellulose benzoates (Figure 6a) *always showed a singlet* at δ ca 2.00 ppm, characteristic of the acetate methyl group. From these spectra, we calculated DS_{Ac} and DS_{Bz} as shown in the last two columns of entries 3 and 4. That is, cellulose acetate was obtained as a by-product when we used RMeImAc-DMSO for the synthesis of cellulose benzoate. Note that the DS_{Ac} in entry 1 is 1.64, i.e., higher than the maximum possible DS_{Ac} of 1.5, see point 2.5 in Experimental. These results suggest that solvent-induced cellulose

acetylation is occurring as a side reaction.

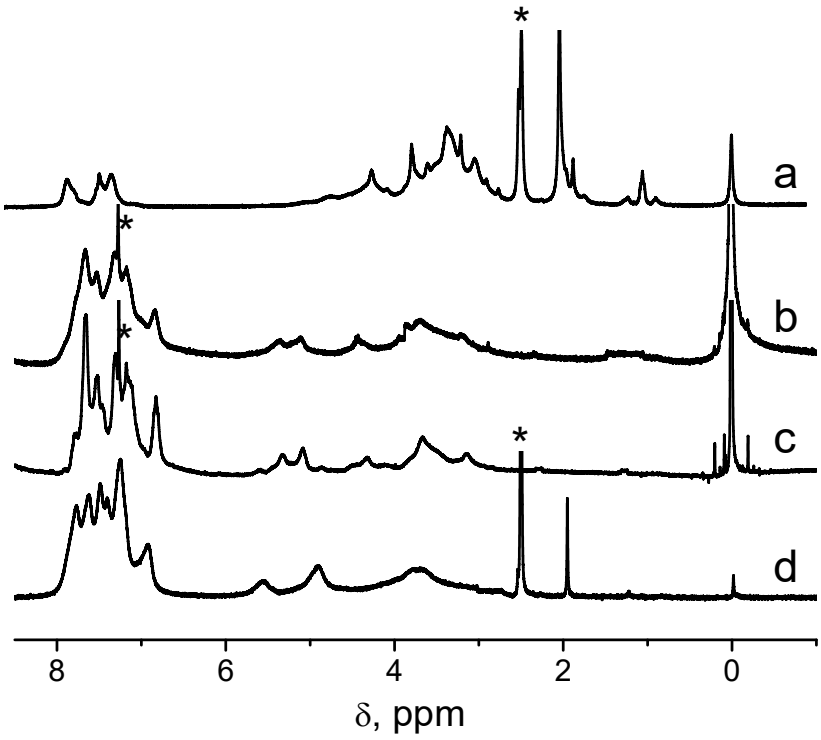

Figure 6. ^{1}H NMR spectra (300 MHz for ^{1}H) of cellulose benzoate: (a) synthesized in C_3OMeImAc-DMSO using *N*-benzoylimidazole as acylating reagent; (b) synthesized in 1-allyl-3-methylimidazolium chloride using benzoic anhydride as acylating reagent; (c) the product synthesized in (b) after stirring with *pure* C_3OMeImAc; (d) the product synthesized an in (b) and stirred in C_3OMeImAc-DMSO (χ_{DMSO} 0.6). In all cases, the treatment conditions of Cell-Bz were 2 h, 15 W and 60 ^{o}C. The peaks marked with * correspond to the non-deuterated solvent residue, DMSO (δ= 2.5 ppm) and $CHCl_3$ (δ = 7.2 ppm).

3.2.1. Acetylation of cellulose as a side reaction in RMeImAc

Acetylation of cellulose in IL with acetate anion is known. Köhler et al. (2007) showed that pure cellulose acetate was obtained when the biopolymer was reacted with 2-furoyl- or tosyl chloride in C_2MeImAc (1-ethyl-3-methylimidazolium acetate). These authors suggested that the

acetate from the IL reacts with derivatizing agents forming mixed anhydrides (e.g., acetic-2-furoic anhydride) which act as acylating reagent. Mixed cellulose acetate-propionate, with $DS_{Ac} > DS_{Pr}$ was prepared by reacting cellulose with propionic anhydride in C_2MeImAc due to the formation of acetic-propionic mixed anhydride (Dorn, 2009). Finally, cellulose acetate (*DS* 0.017) was obtained from cellulose/C_2MeImAc solution, even without the addition of an acetylating agent (Karatzos, Edye, & Wellard, 2012). In this case, acetic anhydride is generated, *in situ*, via dehydration of the acetic acid produced by abstraction of the relatively acidic C2-*H* of the imidazolium ring by the acetate ion (Gericke et al., 2012; Sowmiah, Srinivasadesikan, Tseng, & Chu, 2009).

The DS_{Ac} value obtained by Karatzos et al. (2012) is too small to explain the (large) DS_{Ac} values listed for in entries 3 and 4 of Table 2. Considering that the acylating reagent in the benzoylation reaction is *N*-benzoylimidazole, the formation of mixed acetic-benzoic anhydride was discarded. The reason is that the pK_a values in water are 7.1 and 4.75, for imidazole and acetic acid, respectively (CRC Handbook of Chemistry and Physics, 2017). Consequently, the best leaving group in the tetrahedral intermediate formed by attack of the acetate anion (from the IL) on *N*-benzoylimidazole is the acetate group, not imidazole, leading to regeneration of *N*-benzoylimidazole. It appears, therefore that the production of cellulose acetate (entries 3 and 4 of Table 2) is due to a DMSO-mediated catalysis/reaction.

To test this hypothesis, cellulose benzoate with *DS* 2.6 was prepared in pure 1-allyl-3-methylimidazolium chloride, using benzoic anhydride. As shown in Figure 6b, no peak at 2.00 ppm was observed, i.e., pure cellulose benzoate was obtained. We dissolved the cellulose benzoate thus obtained in pure C_3OMeImAc and in C_3OMeImAc-DMSO (χ_{DMSO} 0.6) and kept the solution under the acylation conditions (15 W MW power, 500 rpm, 60 ^{o}C, 2 h), except that no acylating agent was added. We then recovered/purified the esters from both solutions using the workup procedure given in item 2.5 of Experimental; recorded their ^{1}H NMR spectra. As shown in parts (c and d) of Figure 6, the singlet at ca. 2.0 ppm was observed only in the product recovered from C_3OMeImAc-DMSO (Figure 6d). That is, DMSO is catalyzing the formation of cellulose acetate. Although determination of the mechanism of this reaction is beyond the scope

of the present work, this is another manifestation that ILs and their solutions in MSs may not always be "spectators" (Wang, Qin, Mu, Xue, & Gao, 2017).

3.3. A rationale for effect of IL side-chain structure on cellulose dissolution and acylation

Because of the presence of ether linkage in the side-chain of C_3OMeImAc we expected that it should form more hydrogen bond with AGU-***OH*** leading to higher cellulose dissolution than pure C_4MeImAc and C_4MeImAc-DMSO. Additionally, the (expected) higher Lewis basicity of C_3OMeImAc should contribute favorably to cellulose acylation, due to a combination of less biopolymer aggregation in solution and stabilization of the reaction (polar) transition state. However, our data for cellulose dissolution (Figure 5) and acylation (Table 2) showed the opposite behavior, C_4MeImAc is more efficient than C_3OMeImAc.

The attenuation/elimination of the expected side-chain effect of C_3OMeImAc may arise from macroscopic effects; microscopic effects/interactions, or both. As example of the former we studied solution rheology, whereas we assessed microscopic interactions by ^{1}H, ^{13}C NMR spectroscopy and solvatochromic parameters. We present these results below in the order mentioned.

3.3.1. Rheology of IL-DMSO binary mixtures

The Stokes-Einstein equation for rigid sphere is given by:

$$D = k_B T/6\pi\eta a \quad \textbf{(3)}$$

where *"k_B"*, *"a"* and η refer to the Boltzmann constant, particle radius, and viscosity, respectively (Berry, Rice, & Ross, 2000). Equation 3 indicates that the diffusion coefficient (D) in solution is inversely proportional to the viscosity. Lower viscosity is expected to favor cellulose dissolution and derivatization. This expectation (rate increase as a function of decreasing medium viscosity) was verified experimentally for reactions of isomerization (Baba et al., 2006) and Diels-Alder (Khupse & Kumar, 2011; Tiwari & Kumar, 2012) in pure ILs and their mixtures with MSs.

We investigated the rheological behavior of RMeImAc-DMSO binary mixtures at 60 °C (temperature of cellulose dissolution and acylation). The dependence of viscosity (η) on shear

rate (0.01 – 100 s^{-1}) at 60 °C for RMeImAc-DMSO binary mixture with χ_{DMSO} range 0.2 – 0.9 was evaluated; both ILs-DMSO showed a Newtonian behavior (results not shown). As shown in Figure SM3, the mixture viscosity decreases as a function of increasing χ_{DMSO}; mixtures of C_3OMeImAc-DMSO are more viscous than their C_4MeImAc-DMSO counterparts. The dependence of IL-DMSO solution η (χ_{DMSO} 0.0, 0.4, 0.6, 0.8) on the temperature (*T*) was investigated. From these data, we calculated the energy of viscous flow E_{flow} using Arrhenius-type equation (Gericke et al., 2009). As shown in Table SM4 and Figure SM4 solutions of 1 wt% MCC in C_4MeImA-DMSO are less viscous (ca. 4 %) over the range of χ_{DMSO} investigated and show smaller values of E_{flow} (1-2 J/mol).

The rheology data of IL-DMSO binary mixtures show that both viscosity and E_{flow} of C_4MeImAc-DMSO are smaller than the C_3OMeImAc counterpart, indicating that cellulose dissolution should be favored in the C_4MeImAc, and C_4MeImAc-DMSO, in agreement with our cellulose solubility data. Based on the Stokes-Einstein equation, diffusion of the reactants in C_4MeImAc medium are faster which should affect product *DS* favorably, as shown in Table 2.

3.3.2. Assessment of hydrogen bonding by ^{1}H and ^{13}C NMR

We investigated the efficiency of hydrogen bond formation between cellulose and both solvents systems by ^{1}H and ^{13}C NMR spectroscopy. In order to avoid the severe ^{1}H line broadening observed for cellulose solutions in IL-DMSO (Cao et al., 2016; Lu et al., 2017; Zhang et al., 2010) we used cellobiose as a model. The (linear) dependence of the relevant ^{1}H and ^{13}C chemical shifts (δ) of the ILs in DMSO-d_6 on *[cellobiose]* is shown in Figure SM5, whereas the equations that describe this dependence are listed in Table SM5. In absence of cellobiose, the bonds formed are those between hydrogens of the imidazolium cation, the acetate anion and the (S=O) dipole of DMSO. The hydroxyl groups of cellobiose form hydrogen bonds with both ions of the IL and with DMSO; this is manifested by changes in (δ). We dwell here on the magnitude of $\Delta\delta$ rather than its sign, because the latter is the result of changes in the electron density of the atom (due to hydrogen bonding) coupled with changes in diamagnetic shielding/deshielding by the anisotropic acetate ion and (S=O) dipole of DMSO (Lambert & Mazzola, 2011). Changes in diamagnetic shielding/deshielding result from changes in the movements (diffusion, tumbling, etc.) of the ions

and the solvent dipoles due to their interactions with cellobiose; the magnitude of these changes is not known. The slopes of all equations shown in Table SM5 are larger for C_4MeImAc than C_3OMeImAc. That is the strength of hydrogen bonding is larger for the former IL. Additionally, the slope is largest for C2-***H*** and ***C2***, as expected for this relatively acidic site (Alder, Allen, & Williams, 1995; Amyes, Diver, Richard, Rivas, & Toth, 2004).

In conclusion, ^{1}H and ^{13}C NMR data clearly show: *(i)* the formation of hydrogen bonds between the cations of ILs and hydroxyl groups of cellobiose; *(ii)* the strength of these interactions depends on the acidity of the imidazolium carbon atom (C2), hence the attached hydrogen (the slope of C2-***H*** is largest); *(iii)* these interactions are stronger for C_4MeImAc than C_3OMeImAc. As the NMR data *per se* do not offer a clear answer regarding the origin of the dependence of $\Delta\delta$ on the nature of the IL side-chain, we measured Lewis acidity and basicity of ILs-DMSO using solvatochromic probes.

3.3.3. Solvatochromic data of ILs-DMSO solvent systems

Table SM6 shows all solvatochromic data as a function of χ_{DMSO} calculated by use of solvatochromic probes. As argued elsewhere, the "effective Lewis basicity" (= *SB*-*SA*) is a good indicator of the efficiency of ILs as cellulose solvents (Hauru, Hummel, King, Kilpeläinen, & Sixta, 2012). ILs with large *SB* and small *SA* are good solvents.

Figure 7a shows dependence of (*SB*-*SA*) on χ_{DMSO} for both ILs (Figure 7b will be discussed later). The values of (*SB*-*SA*) are almost constant in the χ_{DMSO} range 0.0-0.8 for the two ILs examined, due to a preferential solvation of solvatochromic probes by a component of each medium (Achtel, Jedvert, Kostag, Seoud, & Heinze, 2018; de Jesus, Pires, Scharf, & El Seoud, 2017). Therefore, the maximum dissolution of cellulose at χ_{DMSO} = 0.6 (Figure 5a) cannot be explained solely on the bases of (*SB*-*SA*). On the other hand, C_4MeImAc is associated with higher effective basicity than C_3OMeImAc at any χ_{DMSO}, hence forms stronger hydrogen bonds with the hydroxyl groups of the AGU. This leads, according to this criterion, to more efficient cellulose dissolution by the IL with alky side-chain. This result agrees with our previous data.

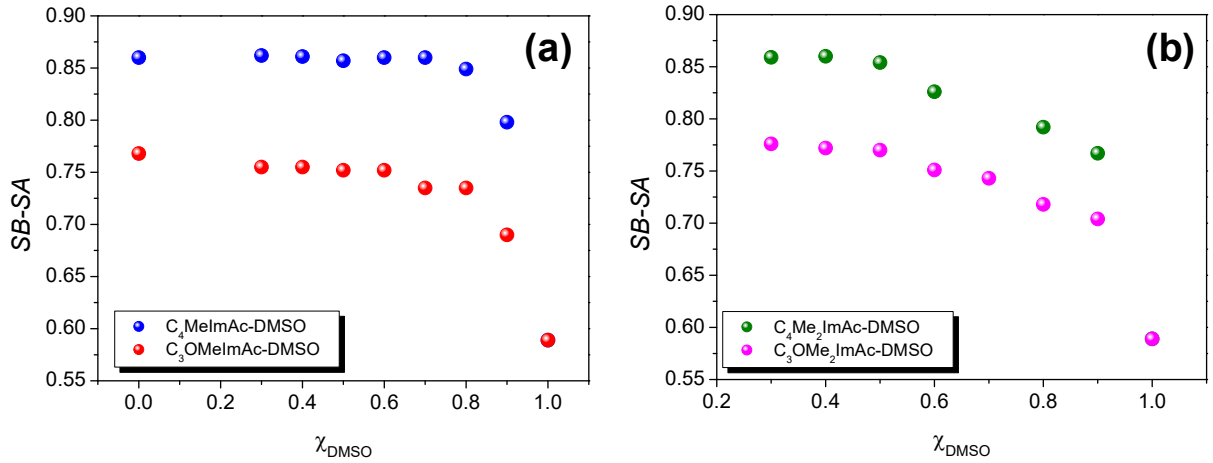

Figure 2. Dependence of effective basicity (*SB-SA*) on DMSO molar fraction (χ_{DMSO}), of RMe_nImAc-DMSO, R = 1-butyl or 2-methoxyethyl, n = 1 (a) or 2 (b), determined at 60 °C.

We now address the reason for the lower efficiency of $C_3OMeImAc$. In a recent publication on solvation by aqueous solutions of $C_4MeImAc$ and $C_3OMeImAc$, we attributed the dependence of solvatochromic parameters on the nature of the side-chain of C_3OMeIm^+ to the formation of intramolecular hydrogen bonding between the ether oxygen with C2-***H*** and C4-***H*** of the imidazolium ring; the former is stronger, see Figure (de Jesus, Pires, Mustafa, Riaz, & El Seoud, 2017). This cycling behavior of C_3OMeIm^+ -indicated by theoretical calculations- was corroborated with ^1H NMR spectroscopy (de Jesus, Pires, Mustafa, et al., 2017). Note that $C_4MeImAc$ is not subject to this side-chain/imidazolium ring hydrogen bonding. Therefore, we attribute the less hydrogen bonding (NMR, Table SM5) and lower effective Lewis basicity (solvatochromism, Table SM6) to the cyclization of C_3OMeIm^+. This intramolecular hydrogen bonding should decrease the interactions of C_3OMeIm^+ OAc^-/cellulose both as hydrogen-bond donor (through the relatively acidic C2-***H***···O(H)-cellulose) and acceptor (cellulose-OH···ether oxygen of the IL side-chain).

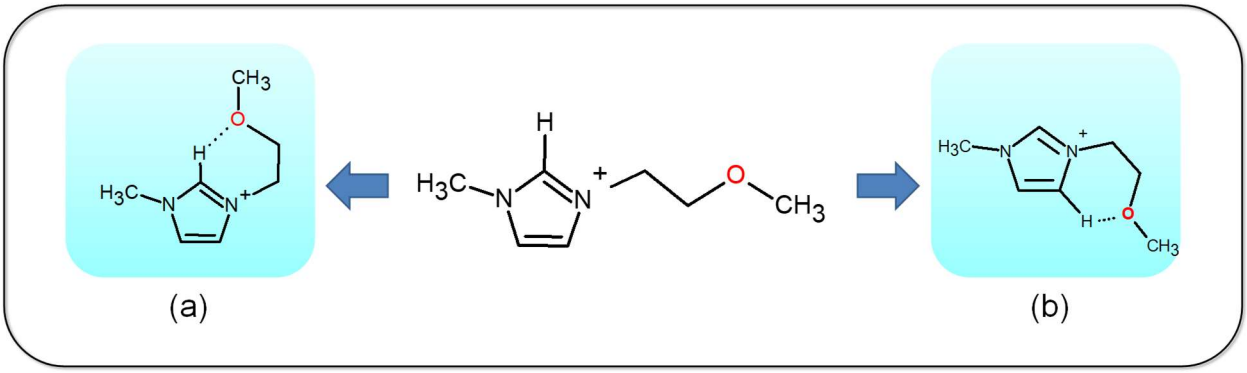

Figure 8. Schematic representation of the possible intramolecular hydrogen bonding in C_3OMeImAc-DMSO between the ether oxygen and C2-***H*** (a) and C5-***H*** (b). These configurations are based on arguments advanced for aqueous solutions of the same ILs (de Jesus, Pires, Mustafa, et al., 2017).

The relevant points of 3.3 are: (i) insertion of ether oxygen in side-chain of IL imidazolium cation did not enhance the dissolution and acylation of the cellulose in that solvent; (ii) both macroscopic and microscopic effects of RMeImAc-DMSO binary mixtures contribute to the observed efficiency of C_4MeImAc.

3.4. Effects of "blocking" position 2 of the imidazolium ring on cellulose dissolution and derivatization

Our recent work on solvatochromism in aqueous solutions of these ILs indicated the following order for empirical polarity: aqueous C_4MeImAc > aqueous C_3OMeImAc. This order was inverted, however, when the IL was based on 1,2-dimethylimidazole, *i.e.*, the order of empirical polarity was: aqueous C_3OMe_2ImAc > aqueous C_4Me_2ImAc (de Jesus, Pires, Scharf, et al., 2017). We decided, therefore, to determine whether 1,2-dimethylimidazole-based ILs are necessarily better solvents for cellulose dissolution and acylation, relative to those based on 1-methylimidazole. As shown in Figure 5b, introduction of C2-***CH_3*** in the imidazolium ring increased the values of wt% dissolved cellulose at every χ_{DMSO}, although C_4Me_2ImAc-DMSO is still a more efficient cellulose solvent than C_3OMe_2ImAc-DMSO, over the entire DMSO concentration range. The enhanced cellulose dissolution by 1,2-dimethylimidazole-based ILs relative to its 1-

457 methylimidazole counterparts may result, in part, from increased solvent-biopolymer
458 hydrophobic interactions because of the slight difference in hydrophobicity of both diazoles
459 (calculated Log P = partition coefficient 1-octanol/water are -0.094 and 0.034 for 1-methyl- and
460 1,2-dimethylimizaole, respectively). However, the ether linkage of the C_3OMe_2Im cation may still
461 form an intramolecular hydrogen bond with C4-***H*** of the imidazolium ring and the weakly acidic
462 hydrogens of the C2-***CH₃*** group, impairing its interaction with cellulose. Note that the C2-***CH₃***
463 hydrogens still undergos H/D exchange, albeit more slowly than the relatively acidic C2-***H*** (Handy
464 & Okello, 2005).

465 Figure 7b shows that the effective Lewis basicity of C_4Me_2ImAc-DMSO solutions is still
466 higher than that of C_3Me_2ImAc-DMSO. Additionally, values of DS_{Ac} of cellulose acetates prepared
467 in both ILs are the same within the uncertainty in DS calculation. Therefore, blocking the C2
468 position of two ILs enhanced cellulose dissolution relative to 1-methylimidazole-based ILs, but
469 did not enhance the Lewis effective basicity or cellulose reactivity.
470

471 **4. CONCLUSIONS**

472 We assessed the effects of presence of (basic) ether linkage in the side chain of RMeImAc
473 ILs and their solutions in DMSO on the solubility of cellulose and its acylation. Contrary to our
474 initial expectation, the presence of this ether oxygen did not enhance the efficiency of IL as a
475 solvent or reaction medium for cellulose. We attributed the lower efficiency of $C_3OMeImAc$ to
476 deactivation of both (–O- and C2-***H***) as hydrogen bonding acceptor, and donor respectively due
477 to intramolecular hydrogen bonding or cyclization, as depicted in Figure 8. We corroborated this
478 conclusion by rheology measurements, ^1H, ^{13}C NMR- and solvatochromic data. The observed
479 enhancement of cellulose dissolution due to methylation of C2 position of the imidazolium ring
480 shows the importance of hydrogen bonding and hydrophobic interactions in cellulose chemistry.
481

482 **Acknowledgments**

483 D. C. Ferreira thanks FIPT for PDCE fellowship for her stay at Aalto University. M. L. Oliveira,
484 T. A. Bioni and H. Nawaz thanks FIPT, Capes, and FAPESP, respectively for their fellowships. O. A.

El Seoud thanks CNPq for research productivity fellowships (grant 307022/2014-5) and FAPESP for financial support (2014/22136-4). H. Sixta and M. Hummel wish to thank Tekes – the Finnish Funding Agency for Innovation - and Finnish Bioeconomy Cluster FIBIC Ltd for funding.

REFERENCES

Achtel, C., Jedvert, K., Kostag, M., Seoud, O. A. El, & Heinze, T. (2018). Surprising Insensitivity of Homogeneous Acetylation of Cellulose Dissolved in Triethyl (n -octyl) ammonium Chloride / Molecular Solvent on the Solvent Polarity, *1800032*, 1–8. http://doi.org/10.1002/mame.201800032

Albright, J. D., & Goldman, L. (1965). Dimethyl Sulfoxide-Acid Anhydride Mixtures. New reagents for oxidation of alcohols. *Journal of the American Chemical Society*, *87*, 4214–4216. http://doi.org/10.1021/ja01096a055

Albright, J. D., & Goldman, L. (1967). Dimethyl Sulfoxide-Acid Anhydride Mixtures for the Oxidation of Alcohols. *Journal of the American Chemical Society*, *89*, 2416–2423. http://doi.org/10.1021/ja00986a031

Alder, R. W., Allen, P. R., & Williams, S. J. (1995). Stable Carbenes as Strong Bases. *Journal of the Chemical Society, Chemical Communications*, *12*, 1267–1268. http://doi.org/10.1039/C39950001267

Amyes, T. L., Diver, S. T., Richard, J. P., Rivas, F. M., & Toth, K. (2004). Formation and Stability of N-Heterocyclic Carbenes in Water: The carbon acid pKa of imidazolium cations in aqueous solution. *Journal of the American Chemical Society*, *126*, 4366–4374. http://doi.org/10.1021/ja039890j

Armarego, W. L., & Chai, C. L. (2009). *Purification of Laboratory Chemicals* (6th ed.). New York: Elsevier Ltd.

Baba, K., Ono, H., Itoh, E., Itoh, S., Noda, K., Usui, T., … Asano, T. (2006). Kinetic Study of Thermal Z to E Isomerization Reactions of Azobenzene and 4-dimethvlaniino-4'-nitroazobenzene in Ionic Liquids [1-R-3- methyliniidazolium

513 bis(trifluoromethylsulfonyl)imide with R = Butyl, Pentyl, and Hexyl]. *Chemistry - A*
514 *European Journal*, *12*, 5328–5333. http://doi.org/10.1002/chem.200600081
515 Berry, R. S., Rice, S. A., & Ross, J. (2000). *Physical Chemistry* (2nd ed.). Oxford: Oxford University
516 Press.
517 Cao, B., Du, J., Du, D., Sun, H., Zhu, X., & Fu, H. (2016). Cellobiose as a Model System to Reveal
518 Cellulose Dissolution Mechanism in Acetate-Based Ionic Liquids: Density functional theory
519 study substantiated by NMR spectra. *Carbohydrate Polymers*, *149*, 348–356.
520 http://doi.org/10.1016/j.carbpol.2016.04.128
521 Casarano, R., Nawaz, H., Possidonio, S., Da Silva, V. C., & El Seoud, O. A. (2011). A convenient
522 Solvent System for Cellulose Dissolution and Derivatization: Mechanistic aspects of the
523 acylation of the biopolymer in tetraallylammonium fluoride/dimethyl sulfoxide.
524 *Carbohydrate Polymers*, *86*, 1395–1402. http://doi.org/10.1016/j.carbpol.2011.06.051
525 Catalán, J., Díaz, C., López, V., Pérez, P., De Paz, J.-L. G., & Rodríguez, J. G. (1996). A Generalized
526 Solvent Basicity Scale: The solvatochromism of 5-nitroindoline and its homomorph 1-
527 methyl-5-nitroindoline. *Liebigs Annalen*, *1996*, 1785–1794.
528 Catalan, J., Mena, E., Meutermans, W., & Elguero, J. (1992). Solvatochromism of a typical
529 merocyanine: stilbazolium betaine and its 2,6-di-tert-butyl derivative. *The Journal of*
530 *Physical Chemistry*, *96*, 3615–3621. http://doi.org/10.1021/j100188a013
531 Ciacco, G. T., Morgado, D. L., Frollini, E., Possidonio, S., & El Seoud, O. A. (2010). Some Aspects
532 of Acetylation of Untreated and Mercerized Sisal Cellulose. *Journal of the Brazilian*
533 *Chemical Society*, *21*, 71–77. http://doi.org/10.1590/S0103-50532010000100012
534 CRC Handbook of Chemistry and Physics. (2017). *CRC* (98th ed.). (J. Rumble, Ed.). CRC press,
535 Boca raton.
536 de Jesus, J. C., Pires, P. A. R., Mustafa, R., Riaz, N., & El Seoud, O. A. (2017). Experimental and
537 Theoretical Studies on Solvation in Aqueous Solutions of Ionic Liquids Carrying Different
538 Side Chains: The n-butyl-group versus the methoxyethyl group. *RSC ADVANCE*, *7*, 15952–
539 15963. http://doi.org/10.1039/C7RA00273D
540 de Jesus, J. C., Pires, P. A. R., Scharf, M., & El Seoud, O. A. (2017). Solvation by Aqueous

Solutions of Imidazole-Based Ionic Liquids: 2- A comparison between alkyl and alkoxy side-chains. *Fluid Phase Equilibria*, *451*, 48–56. http://doi.org/10.1016/j.fluid.2017.08.004

Dorn, S. (2009). *Ionische Flüssigkeiten: neueartige Löse- und Reaktionsmedien in der Cellulosechemie*. *Friedrich-Schiller-Universität Jena*. Friedrich-Schiller-Universität Jena.

Eichinger, D. (2012). A vision of the world of cellulosic fibers in 2020. *Lenzinger Berichte*, *90*, 1–7. Retrieved from http://www.lenzing.com/fileadmin/template/pdf/konzern/lenzinger_berichte/ausgabe_90_2012/LB_2012_1_Eichinger.pdf

El Seoud, O. A., da Silva, V. C., Possidonio, S., Casarano, R., Arêas, E. P. G., & Gimenes, P. (2011). Microwave-assisted derivatization of cellulose, 2 - The surprising effect of the structure of ionic liquids on the dissolution and acylation of the biopolymer. *Macromolecular Chemistry and Physics*, *212*, 2541–2550. http://doi.org/10.1002/macp.201100348

El Seoud, O. A., Nawaz, H., & Arêas, E. P. G. (2013). Chemistry and Applications of Polysaccharide Solutions in Strong Electrolytes/Dipolar Aprotic Solvents: An overview. *Molecules*, *18*, 1270–1313. http://doi.org/10.3390/molecules18011270

Gericke, M., Fardim, P., & Heinze, T. (2012). Ionic Liquids - Promising but challenging solvents for homogeneous derivatization of cellulose. *Molecules*, *17*, 7458–7502. http://doi.org/10.3390/molecules17067458

Gericke, M., Liebert, T., El Seoud, O. A., & Heinze, T. (2011). Tailored media for homogeneous cellulose chemistry: Ionic liquid/co-solvent mixtures. *Macromolecular Materials and Engineering*, *296*, 483–493. http://doi.org/10.1002/mame.201000330

Gericke, M., Schlufter, K., Liebert, T., Heinze, T., & Budtova, T. (2009). Rheological Properties of Cellulose/Ionic Liquid Solutions: From dilute to concentrated states. *Biomacromolecules*, *10*, 1188–1194.

Gericke, M., Trygg, J., & Fardim, P. (2013). Functional Cellulose Beads : Preparation , Characterization , and Applications. *Chemical Reviews*, *113*, 4812–4836. http://doi.org/10.1021/cr300242j

Hämmerle, F. M. (2011). The Cellulose Gap (the Future of Cellulose Fibres). *Lenzinger Berichte*,

89, 12–21.

Handy, S. T., & Okello, M. (2005). The 2-Position of Imidazolium Ionic Liquids : Substitution and Exchange. *Journal of Organic Chemistry*, *13902*(8), 1915–1918. http://doi.org/10.1021/jo0480850

Hauru, L. K. J., Hummel, M., King, A. W. T., Kilpeläinen, I., & Sixta, H. (2012). Role of solvent parameters in the regeneration of cellulose from ionic liquid solutions. *Biomacromolecules*, *13*(9), 2896–2905. http://doi.org/10.1021/bm300912y

Heinze, T., Dicke, R., Koschella, A., Kull, A. H., Klohr, E. A., & Koch, W. (2000). Effective Preparation of Cellulose Derivatives in a New Simple Cellulose Solvent. *Macromolecular Chemistry and Physics*, *201*, 627–631. http://doi.org/10.1002/(SICI)1521-3935(20000301)201:6<627::AID-MACP627>3.0.CO;2-Y

Jedvert, K., & Heinze, T. (2017). Cellulose modification and shaping - A review. *Journal of Polymer Engineering*, *37*(9), 845–860. http://doi.org/10.1515/polyeng-2016-0272

Karatzos, S. K., Edye, L. A., & Wellard, R. M. (2012). The Undesirable Acetylation of Cellulose by the Acetate Ion of 1-ethyl-3-methylimidazolium Acetate. *Cellulose*, *19*, 307–312. http://doi.org/10.1007/s10570-011-9621-0

Khupse, N. D., & Kumar, A. (2011). The Cosolvent-Directed Diels-Alder Reaction in Ionic Liquids. *Journal of Physical Chemistry A*, *115*, 10211–10217. http://doi.org/10.1021/jp205181e

Köhler, S., Liebert, T., Schöbitz, M., Schaller, J., Meister, F., Günther, W., & Heinze, T. (2007). Interactions of Ionic Liquids With Polysaccharides 1. Unexpected acetylation of cellulose with 1-ethyl-3-methylimidazolium acetate. *Macromolecular Rapid Communications*, *28*, 2311–2317. http://doi.org/10.1002/marc.200700529

Kostag, M., & El Seoud, O. A. (2019). Dependence of cellulose dissolution in quaternary ammonium-based ionic liquids/DMSO on the molecular structure of the electrolyte. *Carbohydrate Polymers*, *205*, 524–532. http://doi.org/10.1016/j.carbpol.2018.10.055

Kostag, M., Jedvert, K., Achtel, C., Heinze, T., & El Seoud, O. (2018). Recent Advances in Solvents for the Dissolution, Shaping and Derivatization of Cellulose: Quaternary Ammonium Electrolytes and their Solutions in Water and Molecular Solvents. *Molecules*, *23*,

597 doi:10.3390/molecules23030511. http://doi.org/10.3390/molecules23030511
598 Kuzmina, O., Sashina, E., Troshenkowa, S., & Wawro, D. (2010). Dissolved state of cellulose in
599 ionic liquids - the impact of water. *Fibres and Textiles in Eastern Europe*, *80*, 32–37.
600 Lambert, J. B., & Mazzola, E. P. (2011). *Nuclear Magnetic Resonance Spectroscopy: An*
601 *Introduction to Principles, Applications, and Experimental Methods*. New Jersey: Pearson
602 Education Inc.
603 Laus, G., Bentivoglio, G., Schottenberger, H., Kahlenberg, V., Kopacka, H., Roeder, T., & Sixta, H.
604 (2005). Ionic Liquids: Current Dev Elopments, Potential and Drawbacks for Industr Ial
605 Applications. *Lenzinger Berichte*, *84*(January), 71–85.
606 http://doi.org/10.2174/157017905774322640
607 Lindman, B., Medronho, B., Alves, L., Costa, C., Edlund, H., & Norgren, M. (2017). The relevance
608 of structural features of cellulose and its interactions to dissolution, regeneration, gelation
609 and plasticization phenomena. *Physical Chemistry Chemical Physics*, *19*(35), 23704–23718.
610 http://doi.org/10.1039/c7cp02409f
611 Lu, F., Zhang, C., Lu, B., Yu, K., Liu, J., Kang, H., … Lan, G. (2017). Cellobiose as a model
612 compound for cellulose to study the interactions in cellulose/lithium chloride/N-methyl-2-
613 pyrrolidone systems. *Cellulose*, *24*, 1621–1629. http://doi.org/10.1007/s10570-017-1213-1
614 Marx, M., & Tidwell, T. T. (1984). Reactivity-selectivity in the swern oxidation of alcohols using
615 dimethyl sulfoxide-oxalyl chloride1. *Journal of Organic Chemistry*, *49*, 788–793.
616 http://doi.org/10.1021/jo00179a009
617 Medronho, B., Romano, A., Miguel, M. G., Stigsson, L., & Lindman, B. (2012). Rationalizing
618 cellulose (in)solubility: Reviewing basic physicochemical aspects and role of hydrophobic
619 interactions. *Cellulose*, *19*, 581–587. http://doi.org/10.1007/s10570-011-9644-6
620 Nagel, M. C. V, & Heinze, T. (2012). Study about the efficiency of esterification of cellulose
621 under homogenous condition: dependence on the chain length and solvent. *Lenzinger*
622 *Berichte*, *90*, 85–92.
623 Nawaz, H., Pires, P. A. R., & El Seoud, O. A. (2013). Kinetics and mechanism of imidazole-
624 catalyzed acylation of cellulose in LiCl/N,N-dimethylacetamide. *Carbohydrate Polymers*, *92*,

997–1005. http://doi.org/10.1016/j.carbpol.2012.10.009

Omura, K., & Swern, D. (1978). Oxidation of alcohols by “activated” dimethyl sulfoxide. a preparative, steric and mechanistic study. *Tetrahedron*, *34*, 1651–1660. http://doi.org/10.1016/0040-4020(78)80197-5

Östlund, Å., Lundberg, D., Nordstierna, L., Holmberg, K., & Nydén, M. (2009). Dissolution and gelation of cellulose in TBAF/DMSO solutions: The roles of fluoride ions and water. *Biomacromolecules*, *10*, 2401–2407. http://doi.org/10.1021/bm900667q

Papanyan, Z., Roth, C., Wittler, K., Reimann, S., & Ludwig, R. (2013). The dissolution of polyols in salt solutions and ionic liquids at molecular level: Ions, counter ions, and hofmeister effects. *ChemPhysChem*, *14*, 3667–3671. http://doi.org/10.1002/cphc.201300465

Pires, P. A. R., Malek, N. I., Teixeira, T. C., Bioni, T. A., Nawaz, H., & El Seoud, O. A. (2015). Imidazole-catalyzed esterification of cellulose in ionic liquid/molecular solvents: A multi-technique approach to probe effects of the medium. *Industrial Crops and Products*, *77*, 180–189. http://doi.org/10.1016/j.indcrop.2015.08.015

Possidonio, S., Fidale, L. C., & El Seoud, O. A. (2009). Microwave-Assisted Derivatization of Cellulose in an Ionic Liquid: An efficient, expedient synthesis of simple and mixed carboxylic esters. *Journal of Polymer Science, Part A: Polymer Chemistry*, *48*, 134–143. http://doi.org/10.1002/pola.23770

Rosenau, T., Hofinger, A., Potthast, A., & Kosma, P. (2003). On the conformation of the cellulose solvent N-methylmorpholine-N-oxide (NMMO) in solution. *Polymer*, *44*, 6153–6158. http://doi.org/10.1016/S0032-3861(03)00663-3

Sowmiah, S., Srinivasadesikan, V., Tseng, M.-C., & Chu, Y.-H. (2009). On the chemical stabilities of ionic liquids. *Molecules*, *14*, 3780–3813. http://doi.org/10.3390/molecules14093780

Tiwari, S., & Kumar, A. (2012). Viscosity dependence of intra- and intermolecular Diels-Alder reactions. *Journal of Physical Chemistry A*, *116*, 1191–1198. http://doi.org/10.1021/jp208989z

Wang, B., Qin, L., Mu, T., Xue, Z., & Gao, G. (2017). Are Ionic Liquids Chemically Stable? *Chemical Reviews*, *117*, 7113–7131. http://doi.org/10.1021/acs.chemrev.6b00594

Wei, W., Meng, F., Cui, Y., Jiang, M., & Zhou, Z. (2017). Room temperature dissolution of cellulose in tetra-butylammonium hydroxide aqueous solvent through adjustment of solvent amphiphilicity. *Cellulose*, *24*, 49–59. http://doi.org/10.1007/s10570-016-1113-9

Zhang, J., Zhang, H., Wu, J., Zhang, J., He, J., & Xiang, J. (2010). NMR spectroscopic studies of cellobiose solvation in EmimAc aimed to understand the dissolution mechanism of cellulose in ionic liquids. *Physical Chemistry Chemical Physics*, *12*, 1941–1947. http://doi.org/10.1039/c001176m